STUDY OF AN ACTIVE RC LINE IN THE MICROWAVE REGION

by
Ronald Edward Musiak

Thesis submitted to the Graduate Faculty of the

Virginia Polytechnic Institute

in partial fulfillment for the degree of

MASTER OF SCIENCE
in

Electrical Engineering

APPROVED:

Chairman Dr. T. P. Kabaservice

Dr. C. A. Holt

Dr. H. L. Krauss

Dr. W. A. Blackwell

JUNE 1970

Blacksburg, Virginia

7-20-77

ACKNOWLEDGMENTS

The author would like to take this opportunity to thank three men largely responsible for the work done in this thesis. Thanks go to

for providing the idea and the device he designed. He was of great assistance in providing theoretical and technical information related to his design. Thanks also go to

and whose approaches to circuit synthesis and semiconductor electronics were of great value and utility. This author greatly appreciates what these men have done for him.

This thesis is dedicated to whose love and devotion was a constant source of encouragement during this time.

TABLE OF CONTENTS

FIGURES AND TABLES

FIGURES

TABLES

THEORY

Negative Conductance Effects Through Avalanche

The original work done in obtaining negative conductance through the mechanism of an avalanching p-n junction was by W.T. Read, Jr. [1] His theory laid the foundation for continued investigations by T. Misawa [2], who designed two Si structures based on a modified version of Read's theories. Misawa called his diode structures AVX-1 and AVX-2. The AVX-1 approximated the structure of Read's diode (abrupt junction where avalanche multiplication occurred evenly across the junction surface). The AVX-2 used a hybrid of an abrupt and linear-graded junction. The AVX-1 structure was used in the design of the active RC line of this thesis. Therefore discussion will be limited to theory of operation and application of the AVX-1 structure.

The AVX-1 (or IMPATT diode as it will be referred to from now on) produces a negative conductance effect in the following manner. Consider a simplified model of the diode shown in figure 1. The junction is reverse biased so that avalanching occurs. The d-c components of current and voltage are represented by I and V respectively; the a-c components by i_s and e_s. The p^+ symbol represents heavy doping of the p material (this doping will be considered high enough relative to the doping of the n material so that the distance ℓ, shown

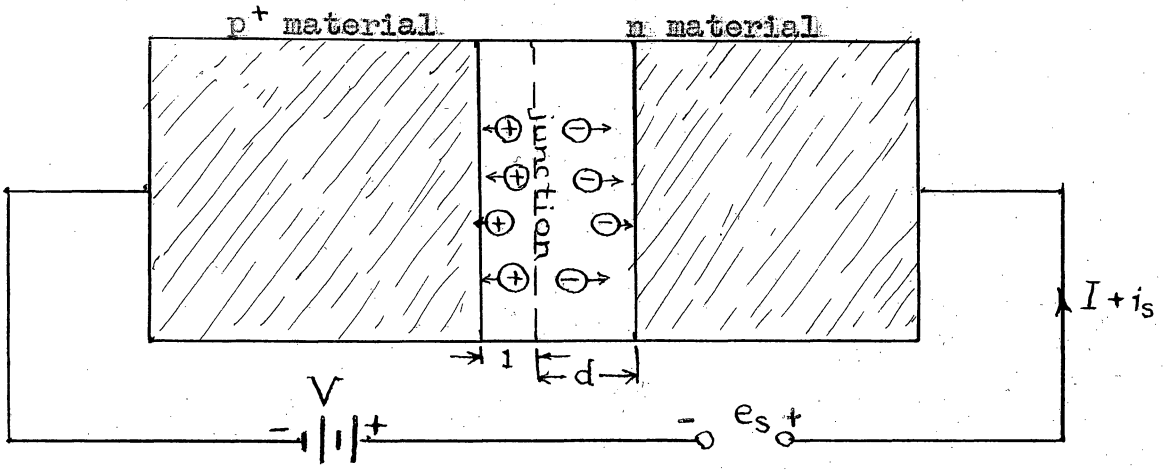

Fig. 1

Model of an IMPATT diode

in the active mode

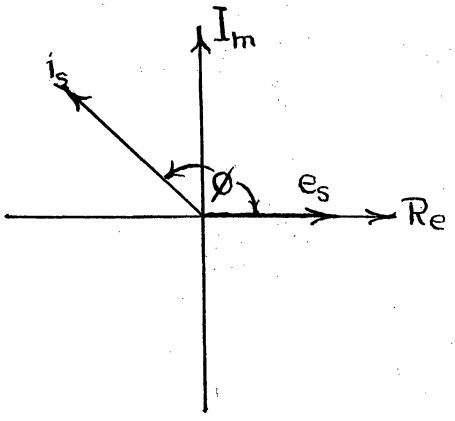

Fig. 2

Phasor diagram showing

delay of i_s relative to e_s

in the figure can be taken to be much, much smaller than the distance d). Under steady-state avalanche conditions it is assumed that in the space-charge region hole and electron velocities are constant and very nearly equal to each other (under this assumption the transit time of holes through distance d can be neglected), changes in carrier densities do not appreciably affect the E-field distribution, and the magnitude of e_s is much, much smaller than V (small-signal conditions). Thus, sinusoidal variations of e_s will produce sinusoidal variations in the E field of the space-charge region. The E-field variations will produce similar variations in carrier densities and these variations will show up in the output current as i_s. However, variations in carrier density originate at the junction where avalanche is taking place. These changes in density must move across the space-charge region (of length d) before they can be seen in the output current. Therefore, a phase delay of i_s relative to e_s is present. If the length of time it takes the electrons to cross the region is greater than a quarter of a cycle of e_s, the impedance of the diode begins to look like a negative conductance shunted by some reactance. This is best illustrated by the phasor diagram in figure 2. For $90^\circ < \phi < 180^\circ$, the diode looks like a negative conductance shunted by a capacitive reactance. For $180^\circ < \phi < 270^\circ$, the reactive part becomes inductive. Optimum negative conductance is obtained when $\phi = 180^\circ$ or when f_s (the frequency of the signal source)

equals 1/2t where t is the transit time of the electrons across the space-charge region. For the particular IMPATT diode used in this thesis, d was given as 5μ and v, the carrier velocity as 10^7 cm/sec [2]. The transit time, found by using the equation $t = 1/v$ with the above values appropriately substituted, is found to be 5×10^{-11} sec. This value of transit time, when substituted into the equation for f_s yields a frequency for optimum negative conductance of 10 GHz. However, in the actual working device, this frequency will be slightly lower because of depletion-layer capacitance which is present in a back-biased diode. Thus, over the frequency range where ϕ falls within the range of 90° to 270°, the avalanche diode can be represented by an equivalent parallel R-L-C network in which R is the negative-real part of the diode's impedance and C includes the depletion-layer capacitance that shunts the network. Also, it is apparent from the above discussion that this "resonant circuit" will exist only if the diode is operated in the microwave region and that both the real part as well as the reactive part of the diode's impedance are a function of frequency.

Two final factors that have to be considered are how the d-c bias supply and amplitude of signal voltage affect the operation of the diode.

It was stated earlier that the resonance frequency (or frequency at which optimum negative conductance occurs) is a function of d. Since d is a function of bias voltage, any change in bias voltage will

affect the diode's resonance frequency. Also, it was found by Read and Misawa that if the current density through the space-charge region was large enough to affect the E-field distribution within that region, the delay of the carriers was reduced. The greater the current density, the shorter the delay. If the current density got high enough, the negative conductance effect disappeared entirely. This observation puts an upper limit on the amount of avalanche current that can go through the diode (aside from heat dissipation considerations). But, below this limit it is possible to "tune" the diode by varying the bias on the diode. The width of the space-charge region as well as the magnitude of the negative conductance can be varied by suitable adjustment of the d-c bias.

Finally, if the amplitude of the signal voltage becomes large enough to cause appreciable modulation of the depletion-layer width, transit-time delay will be affected. Not only does the distance through which the carriers must travel change continuously but the magnitudes of the real and imaginary parts of the diode's impedance become modulated as well. Such effects fall under the heading of parametric operation (see the paper written by DeLoach and Johnston Ref. 3).

Summarizing: the avalanching diode's transit-time delay can be utilized in producing a negative conductance effect (along with a reactive component); the negative-real and reactive components of the

diode are functions of frequency and bias current (and for large signals, a function of signal amplitude also); and the resonance frequency is proportional to the width of the space-charge region and proportional to the square root of the bias current (a second-order effect).

Negative Conductance Networks

The material in this section describes a type of network that makes use of negative conductance components as elements of the network. The general information developed here is coupled with the properties of the avalanche diode later on in order to describe the active RC line designed by Dr. T. P. Kabaservice and used in the experimental work of this thesis.

To begin, consider the two-port network of figure 3. The chain-matrix equations for this network take the form

$$V_1 = AV_2 + BI_2 \tag{1}$$

$$I_1 = CV_2 + DI_2 \tag{2}$$

or in matrix notation

$$\begin{bmatrix} V_1 \\ I_1 \end{bmatrix} = \begin{bmatrix} A & B \\ C & D \end{bmatrix} \begin{bmatrix} V_2 \\ I_2 \end{bmatrix} \tag{3}$$

where

$$A = V_1/V_2\Big|_{I_2=0} = 1 + Z_1/Z_2 \tag{4}$$

$$B = V_1/I_2\Big|_{V_2=0} = Z_1 \tag{5}$$

$$C = I_1/V_2\Big|_{I_2=0} = 1/Z_2 \tag{6}$$

$$D = I_1/I_2\Big|_{V_2=0} = 1 \tag{7}$$

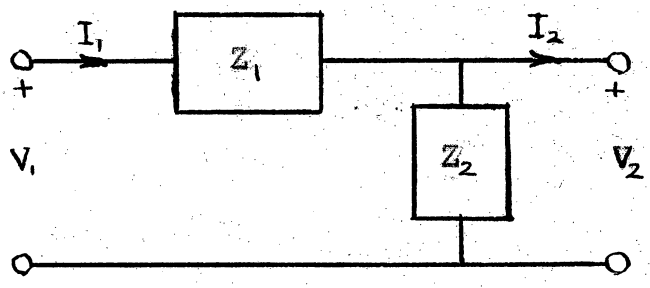

Fig. 3

A generalized two-port network

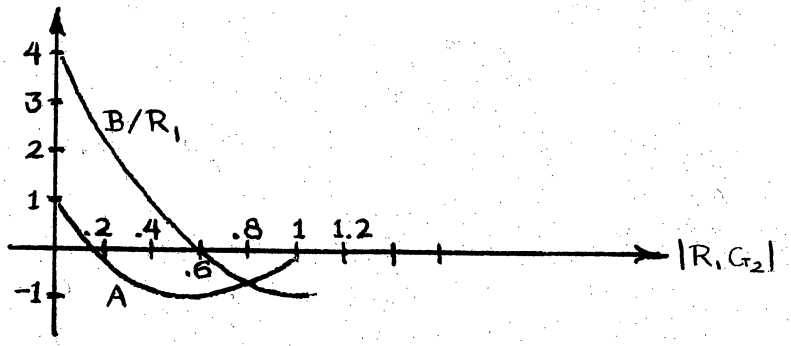

Fig. 4

Plot of B/R_1 and A versus $|R_1 G_2|$

The actual device uses four sections of this network cascaded. For four such sections, the elements of the overall chain matrix are

$$A = X^4 + 7X^3 + 15X^2 + 10X + 1 \tag{8}$$

$$B = Z_1(X^3 + 6X^2 + 10X + 4) \tag{9}$$

$$C = 1/Z_2\,(X^3 + 6X^2 + 10X + 4) \tag{10}$$

$$D = X^3 + 5X^2 + 6X + 1 \tag{11}$$

where $X = Z_1/Z_2 = Z_1 Y_2$. The chain-matrix of the overall network, including a load Y_L can now be found. Starting with

$$\begin{bmatrix} V_1 \\ I_1 \end{bmatrix} = \begin{bmatrix} A & B \\ C & D \end{bmatrix} \begin{bmatrix} 1 & 0 \\ Y_L & 1 \end{bmatrix} \begin{bmatrix} V_2 \\ I_2 \end{bmatrix} \tag{12}$$

the final form becomes

$$\begin{bmatrix} V_1 \\ I_1 \end{bmatrix} = \begin{bmatrix} (A + BY_L) & B \\ (C + DY_L) & D \end{bmatrix} \begin{bmatrix} V_2 \\ I_2 \end{bmatrix} \tag{13}$$

In order to point out some interesting properties of this type of network, the gain expression

$$V_2/V_1 = 1/(A + BY_L) \tag{14}$$

will be used.

CASE I All impedances and admittances are made purely real quantities. Thus, $Z_1 = R_1$, $Y_2 = -G_2$, $Y_L = G_L$ (Note that negative conductance has been introduced into the shunt branches of the network). This negative conductance makes $X = -R_1 G_2$. Substituting this value for X into (8) and (9) yields

$$A = (R_1 G_2)^4 - 7(R_1 G_2)^3 + 15(R_1 G_2)^2 - 10(R_1 G_2) + 1 \qquad (15)$$

$$B = R_1(-(R_1 G_2)^3 + 6(R_1 G_2)^2 - 10(R_1 G_2) + 4) \qquad (16)$$

which are of the same form as those derived by T. P. Kabaservice [4]. Since A and B are functions of the product $-R_1 G_2$, the network gain expression is also a function of that product. To show how this product affects network gain, a plot of A versus $|R_1 G_2|$ and B/R_1 versus $|R_1 G_2|$ was made [4] and is reproduced in figure 4. The present expression for network gain is

$$V_2 / V_1 = 1/(A + BG_L)$$

Therefore, gain is realized if the sum $(A + BG_L)$ is positive and less than unity. This occurs if $|R_1 G_2|$ is less than 0.6 as indicated in figure 4. If $|R_1 G_2|$ is larger than 0.6, the sum $(A + BG_L)$ is negative and this according to stability criteria for the active RC line, makes the line unstable. Also, figure 4 shows that A changes very little for values of $|R_1 G_2|$ between 0.3 and 0.6. Therefore a tolerance range for

$|R_1 G_2|$ can be given as

$$0.3 < |R_1 G_2| < 0.6$$

In the actual device, the value of $|R_1 G_2|$ was taken to be 0.3 because of heat dissipation limits associated with developing the necessary value of $|G_2|$. In the device, $R_1 = 600$ ohms and $|G_2| = 0.5$ mmhos were used to get the product value equal to -0.3.

Substitution -0.3 into the expressions for A and B yields a gain expression of

$$V_2 / V_1 = R_L / (907.8 - .8309 R_L) \qquad (17)$$

Equation (17) reveals that network gain is a function of R_L. For this particular example, the range of R_L for which stable gain occurs is

$$0 < R_L < 1093 \text{ ohms}$$

CASE II In order to check the stability of the network when reactive elements are introduced, Y_2 is modified so that it now equals $-|G_2| + SC_2$ (where S is the Laplace frequency variation). This is done to make the network being developed here more closely resemble the final active RC line. For this substitution for Y_2, the variable X now becomes

$$X = SR_1 C_2 - |R_1 G_2|$$

Use of the expression for the open-circuited voltage gain of the network (no load applied to the output port) yields

$$V_2/V_1 = 1/A = 1/(X^4 + 7X^3 + 15X^2 + 10X + 1)$$

The denominator of this expression is factored to determine the location of its poles in the S-plane. The factored expression is

$$1/A = 1/(X + 0.1206)\cdot(X+1)\cdot(X+2.3473)\cdot(X + 3.5321) \qquad (18)$$

To determine whether or not stable conditions exist, the values of the above poles and the expression $X = SR_1C_2 - |R_1G_2|$ are used.

Stable operation of the network occurs if all the poles of its gain expression lie in the left-half of the S-plane. This condition is met in this case if $|R_1G_2|$ is smaller than 0.1206. However, it has already been stated that the value of $|R_1G_2|$ for the actual device was to be 0.3. Therefore, the active RC line will oscillate under open-circuited conditions or when the value of R_L equals or exceeds 1093 ohms.

Two other parameters of this network that are of interest are the input impedance as seen by a signal source and the power gain.

The input impedance can be found by making use of (1) and (2) (keeping in mind that the elements A, B, C and D are for the total unloaded network). Thus

$$V_1 = AV_2 + BI_2$$

$$I_1 = CV_2 + DI_2$$

but $V_2 = Z_L I_2$, therefore

$$V_1 = AZ_L I_2 + BI_2$$

$$I_1 = CZ_L I_2 + DI_2$$

Taking the ratio $V_1 / I_1 = Z_{in}$

$$Z_{in} = (AZ_L + B)/(CZ_L + D)$$

If all the network components have the real values used in CASE I, the expression for Z_{in} becomes

$$R_{in} = (0.8309R_L - 907.8)/(0.7565x10^{-3}R_L + 0.377) \qquad (19)$$

Since R_L was already defined to have a range of values between 0 and 1093 ohms, the value of R_{in} will remain negative. This is undesirable because connection of a signal source across a negative resistance can lead to oscillatory conditions. This problem can be eliminated by shunting the input of the network with a positive-real resistance R_g, such that $R_g < |R_{in}|$, or from (19), for

$$R_g < (907.8 - 0.8309R_L)/(0.377 + 0.7565x10^{-3}R_L) \qquad (20)$$

By adjusting R_g according to (20), it is possible to make R_{in} take on any positive real value. Thus, the input resistance of the network can be adjusted to match the source resistance in order to obtain an optimum transfer of signal power or to minimize loading a signal source by the network.

The chain-matrix of the network including load and shunt conductance (or admittance) is

$$\begin{bmatrix} V_1 \\ I_1 \end{bmatrix} = \begin{bmatrix} (A + BG_L) & B \\ Y_g(A + BG_L) + (C + DG_L) & (Y_g B + D) \end{bmatrix} \begin{bmatrix} V_2 \\ I_2 \end{bmatrix} \qquad (21)$$

The chain matrix of (21) reveals that the voltage gain of the network is not affected by the addition of the shunt admittance at the input.

The power gain of this network is derived in the following manner. Power gain G_p is defined as

$$G_p = P_{out} / P_{in}$$

where

$$P_{out} = |V_2|^2 / R_L$$

$$P_{in} = |V_{in}|^2 / R_{in}$$

$$V_{in} = R_{in} V_S / (R_{in} + R_S)$$

V_S = source voltage

R_S = source resistance

By use of these relations, the power gain can be expressed as

$$G_p = (1/(A + BG_L))^2 (R_S + R_{in})^2/(R_L R_{in}) \qquad (22)$$

For the condition of maximum power transfer ($R_{in} = R_S$), (22) reduces to

$$G_p = (1/(A + BG_L))^2 (4R_{in})/(R_L)$$

Thus, the negative conductance network has gain which is a function of $-R_1 G_2$ and the load. For the particular device under study, the network will oscillate under open-circuit conditions because $|R_1 G_2|$ is greater than 0.1206. The input resistance of the network can be made positive real by shunting the input with an appropriate positive resistance.

A COMPUTER PROGRAM

A computer program has been designed to predict the performance of the active RC line at its resonance frequency. This mode was chosen because it is at this frequency that the reactive components in the line vanish and the negative conductance is at its optimum value. This mode also allows the computer to work with purely real quantities which simplifies programming. An attempt was made to incorporate reactive elements into the computer circuit model but excessive round-off errors and exponential over-flow conditions gave erroneous results.

The program was designed to allow variation of network parameters either to match the performance of the actual device or to provide answers to ways of optimizing the performance of the device. The program makes use of matrix multiplication to arrive at a final chain-matrix of the complete network. Once this is obtained, the program uses the various elements in the matrix to obtain network voltage gain and input impedance. Input data for the program are the values of the network components, the number of cascaded stages of the network proper, the desired network gain and input impedance (for which the computer will automatically calculate the values of R_g and R_L to fit these conditions). The operator also has the option of reading in R_g and R_L to obtain results on the response of the network to these values.

In either case, the output of the computer gives the values of voltage gain and input impedance as a function of R_g and R_L.

Appendix A contains a listing of the program plus some output data based on the component values obtained from the design data of the actual device.

DESIGN OF THE EXPERIMENTAL DEVICE

*General Considerations

In beginning the design of an active RC line, consideration of the type of active device to be used is of prime importance. The type of active device will determine the frequency range of the line, available negative conductance, characteristic shunt capacitance per line section, resistivity available in direction of transmission and the maximum allowable active area of the line (determined from heat dissipation considerations). Also, how the active device can be built into the rest of the system must be considered.

From these considerations and the present state-of-the-art, the impact avalanche transit-time (IMPATT) diode was selected [4]. Construction of the active RC line using IMPATT diodes is compatible with standard silicon integrated circuit fabrication techniques. Also, because the IMPATT diode exhibits self-resonance, its incorporation into r-f bandpass amplifiers and cavityless oscillators can be studied.

* Design of the active RC line was done by T. P. Kabaservice. UAC Research Labs of East Hartford, Connecticut was the fabricators and suppliers of the line.

Design Of The RC Line

The characteristics of the IMPATT diode used in the experimental device are obtained from the small-signal theory of Misawa's AVX-1 structure [2]. This structure consists of a 6μ thick epitaxial layer of 5 ohm-cm n-type material on an n^+ substrate. A p^+ diffusion is made into the epitaxial layer to form the avalanche junction. Under avalanche conditions, the junction is about 5 μ thick. The sustaining voltage for avalanche is approximately 80 volts and the current density in the junction is about 1.36×10^3 amps/cm . The total area of the avalanching junction was to be 4.6×10^{-5} cm and the total available negative conductance for this area was found to be 2.07×10 mho (see pages 6 and 7 of Ref. 4). Since the RC line consists of four identical sections, the negative conductance available for each section becomes approximately 0.5 mmho. In order to obtain the value of 0.3 for $|R_1 G_2|$, R_1 (resistor diffusion) must be 600 ohms. Considerations in fabricating the RC line into a single monolithic structure are: maintaining high E fields only within the active regions, keeping parasitic shunt capacitance to a minimum and obtaining uniform avalanche across the active region. Refer to pages 7 through 14 of reference 4 for the details. Also, there are problems in connecting the chip to the "outside world". Connections for biasing were brought out from the chip to its housing

by gold wire. Isolation of r-f from the d-c biasing lines was accomplished by diffusing an n electrostatic shield through the epitaxial layer. Connections for r-f between the edges of the chip and the RC network within the chip are microstrip transmission lines. The upper conductor of these lines is evaporated aluminum on the epitaxial layer. The lower conductor is the n substrate shorted to the metal header upon which the chip is mounted. The dielectric of these lines is the epitaxial layer. Connection of these lines to the r-f leads of the header is made with gold ribbon. Since attenuation in the dielectric of the coupling lines is rather high, (on the order of a few db) the p^- resistor diffusion was extended to cover the area of the upper conductor of the input and output lines (for the "shorted fingers" chip only - to be explained later). This diffusion extension made the region of the epitaxial layer between the line conductors have the sustaining voltage of the active regions across it with the result that the line dielectric becomes a space-charge region with reduced conductivity and reduced r-f attenuation. On succeeding pages are sketches of the physical layout of the chip (figure 5) and the chip mounted to its holder (figure 6) as well as photomicrographs of the two types of mounted chips used for experimentation (plates 1 and 2).

The difference between the two types of chip is the way the d-c biasing is applied to the diode sections. In one chip the aluminum bias

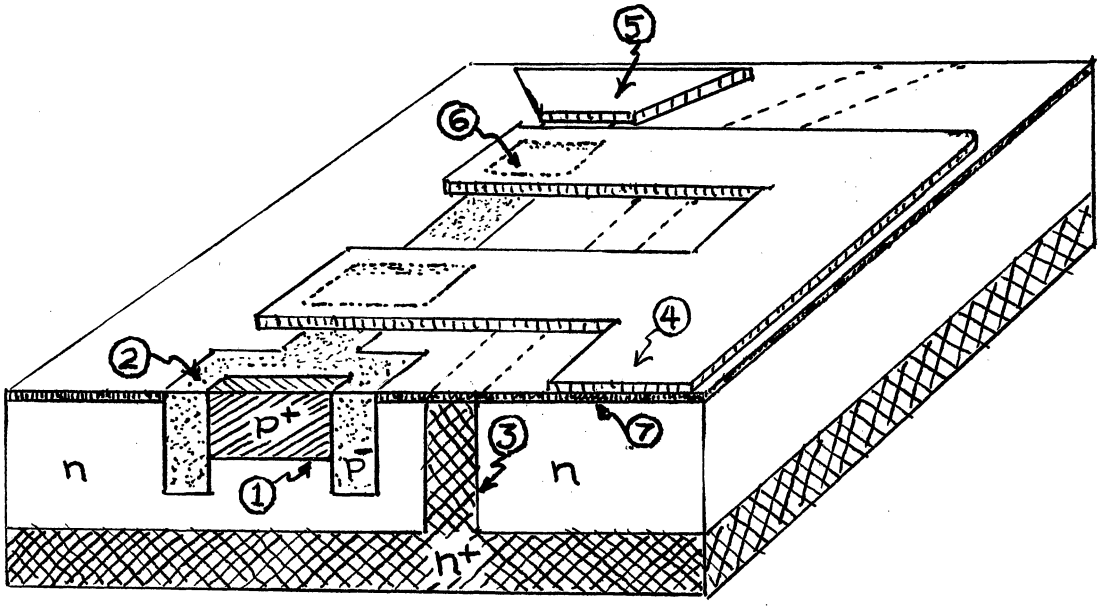

Fig. 5

Cutaway section of chip showing 1) avalanche junction 2) resistor diffusion as "guard-ring" structure 3) n^+ electrostatic shield 4) aluminum contact fingers for biasing 5) aluminized resistor diffusion extension 6) connection to p^+ diffusion 7) SiO_2 insulation

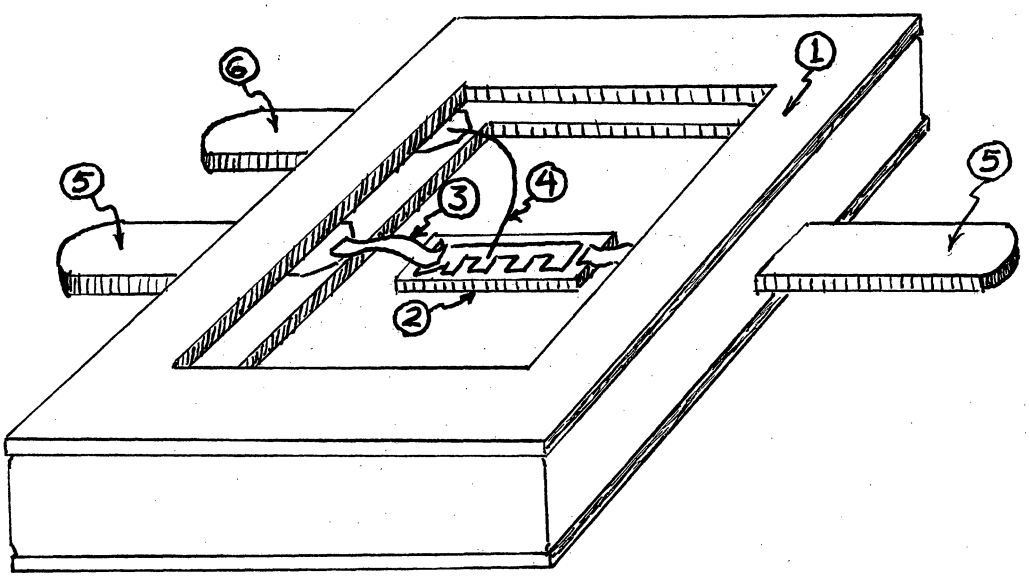

Fig. 6

Sketch of chip mounted to header showing 1) header 2) chip 3) gold strip line 4) gold thread for d-c biasing 5) input and output r-f tabs 6) d-c bias tab

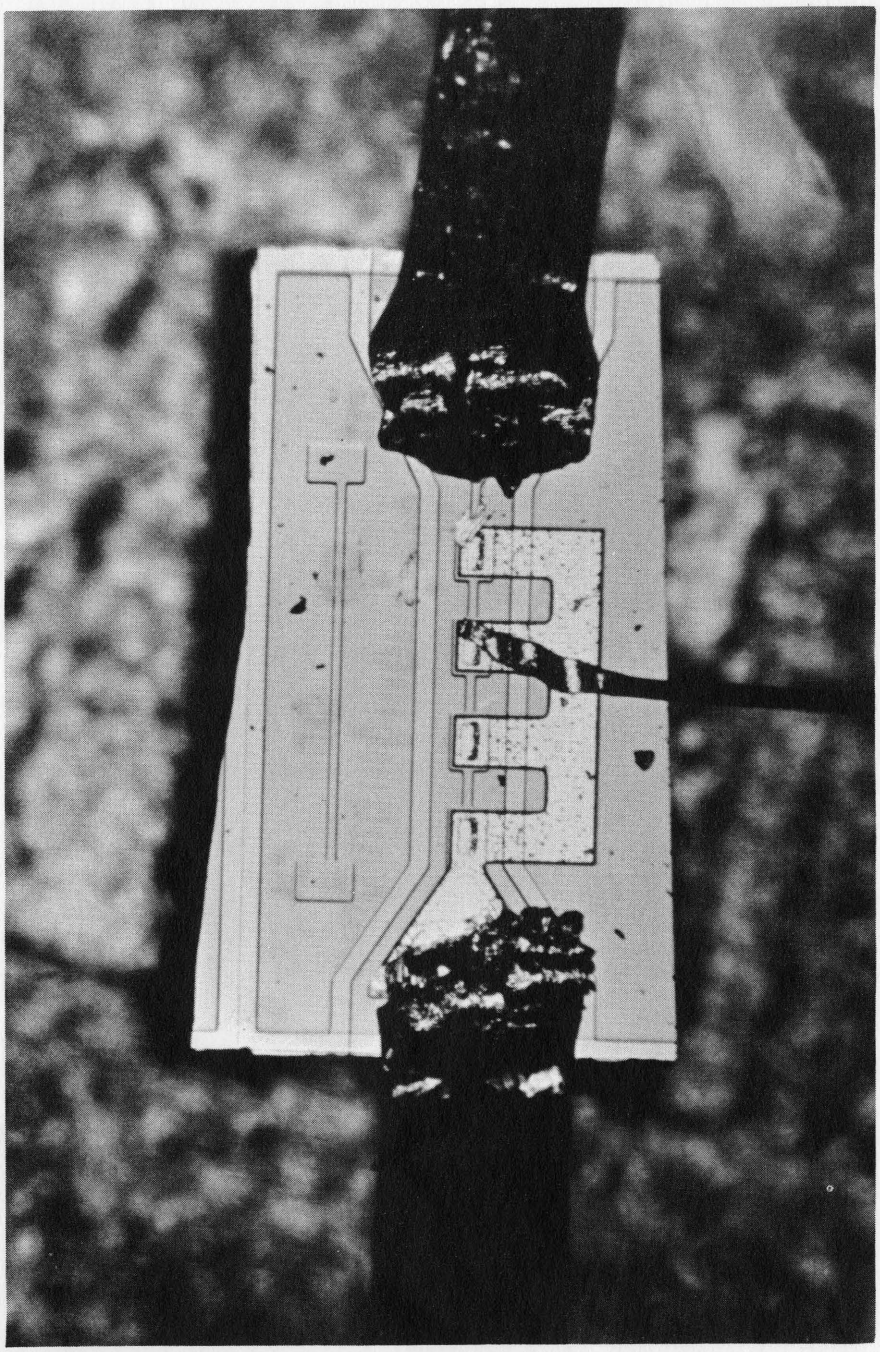

PLATE 1
X150 MAGNIFICATION
OF CHIP

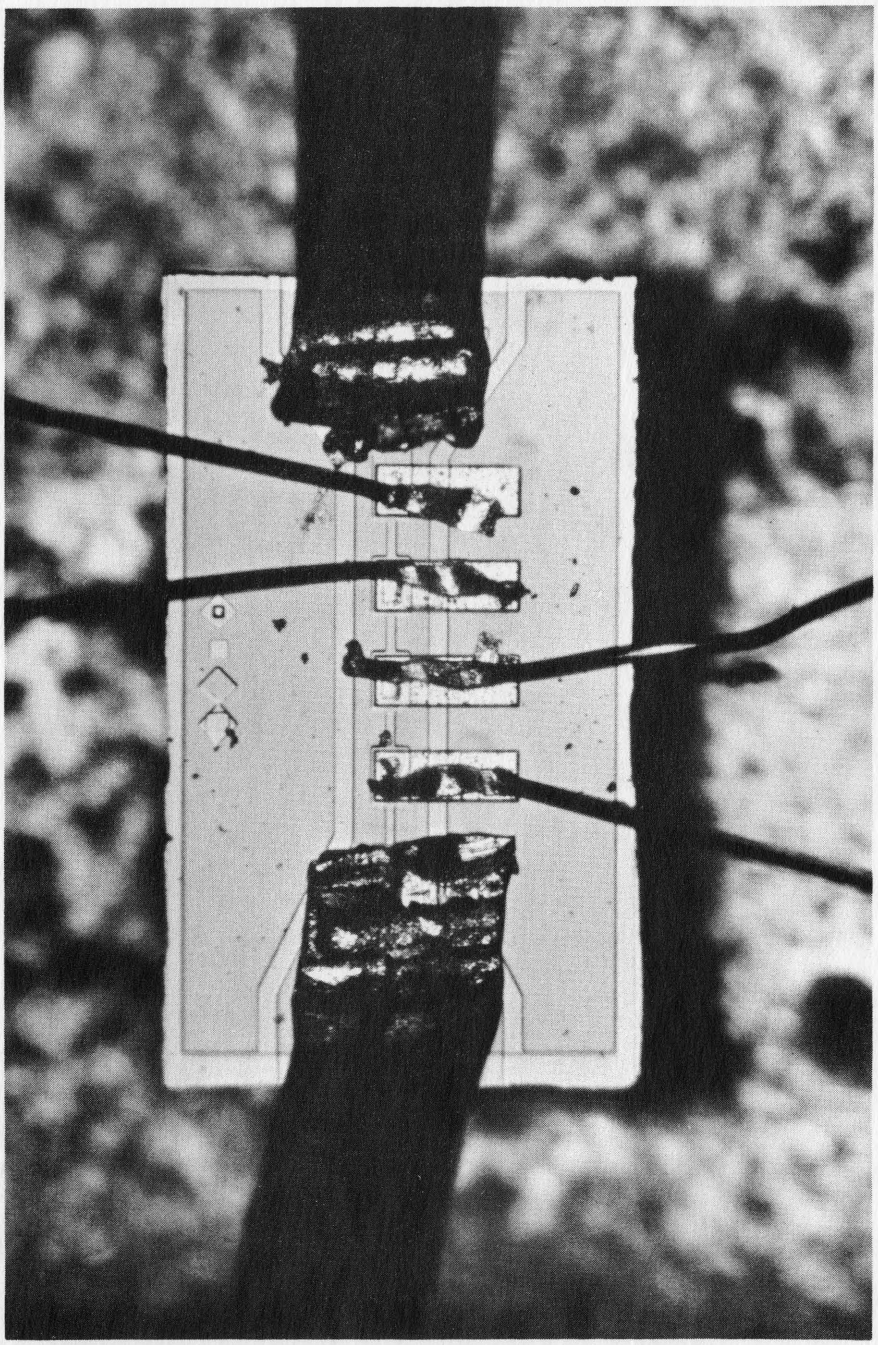

PLATE 2
X150 MAGNIFICATION
OF CHIP

fingers are connected together and the aluminum plating on one of the resistor diffusion extensions is connected to the biasing fingers on the output r-f side (the "shorted fingers" chip mentioned earlier). On the other chip the biasing fingers are separate and there is no connection to these fingers of the aluminum plating of either extension. Both arrangements were used to study the various characteristics of the chip. Figure 7 is a schematic representation of the active RC line. The r-f chokes shown in the figure represent the inductive reactance of the biasing fingers. The shunt capacitor C is the capacity between the biasing strip and the n^+ electrostatic shield. The effect these elements have on the line is to prevent the r-f signal being shunted to ground through the bias supply.

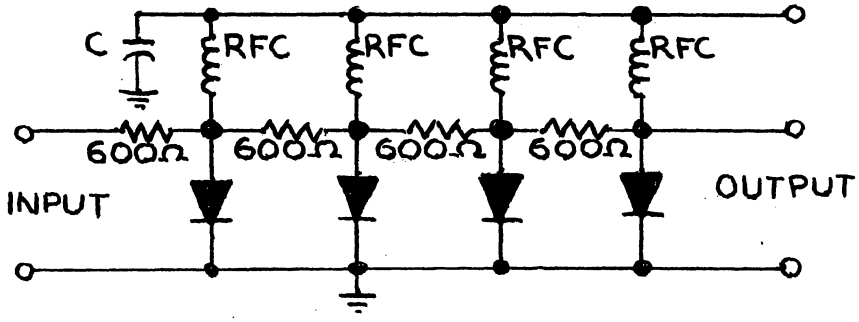

Fig. 7

Schematic diagram of the active RC line

EXPERIMENTAL WORK

Hardware Details Associated With The Device

In order to test the active RC line as part of a microwave system, a method had to be devised to couple r-f into and out of the RC line as well as providing a means of biasing the device. The r-f connections were made by a holder designed by H. W. Glick of UAC Research Labs. Its construction is shown in figure 8. The holder was made of Teflon (top piece) and copper (bottom piece). An OSM-type connector (① and ②) provided the r-f coupling. The center pins of the connectors were flattened so that they could rest on top of the r-f tabs of the header (see figure 6). The r-f tabs and center pins were clamped together by pressure screws (③ and ④). The r-f connections were prevented from shorting to the copper block by small Teflon inserts (⑤ and ⑥). The OSM connectors were held in place by four screws and the entire assembly bolted together holding the header (⑦) in place as shown. It was noted that the pressure screws affected line performance so small pieces of Bakelite were inserted between the pressure screws and the r-f tabs to minimize this effect.

The transition from waveguide to OSM connector was accomplished as shown in figure 9. This particular arrangement had to be used

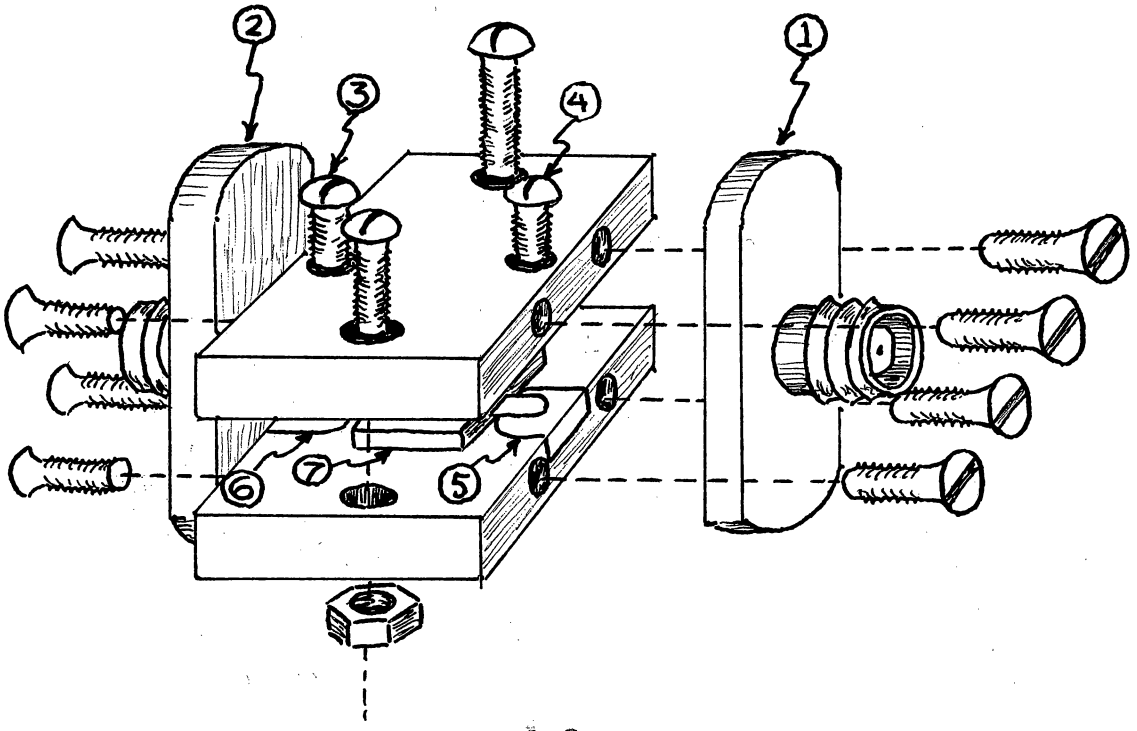

Fig. 8

Exploded view of holder

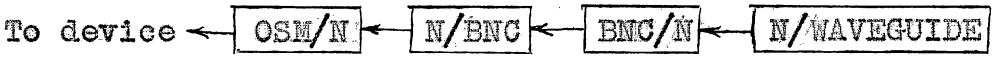

Fig. 9

Block diagram of transition connectors

because it was the only one available and was used only in going from the signal source end to the device. In going from the device to the rest of the set-up, an OSM/N and N/WAVEGUIDE transition was all that was necessary.

Connections for biasing the device were made by soldering a length of wire directly to the bias tab of the header for V^- and connecting the ground return lead to the copper block of the holder. A photograph of this portion of the assembly is shown on the next page. The rest of the bench assembly will be described as various tests on the device are described. Below is a listing of the equipment used in this experiment.

EQUIPMENT

1. Tektronix Oscilloscope
2. GR Pulse Generator
3. Heathkit DC Supply
4. Wavetek VCG
5. HP Power Meter
6. HP SWR Meter
7. HP Klystron Supply
8. 723 A/B Klystron
9. Western Elec. Isolator
10. HP Wavemeter
11. HP Precision Atten.
12. Slide-Screw Tuner
13. Slotted Line
14. Microammeter
15. Waveguide, Connectors, Cable

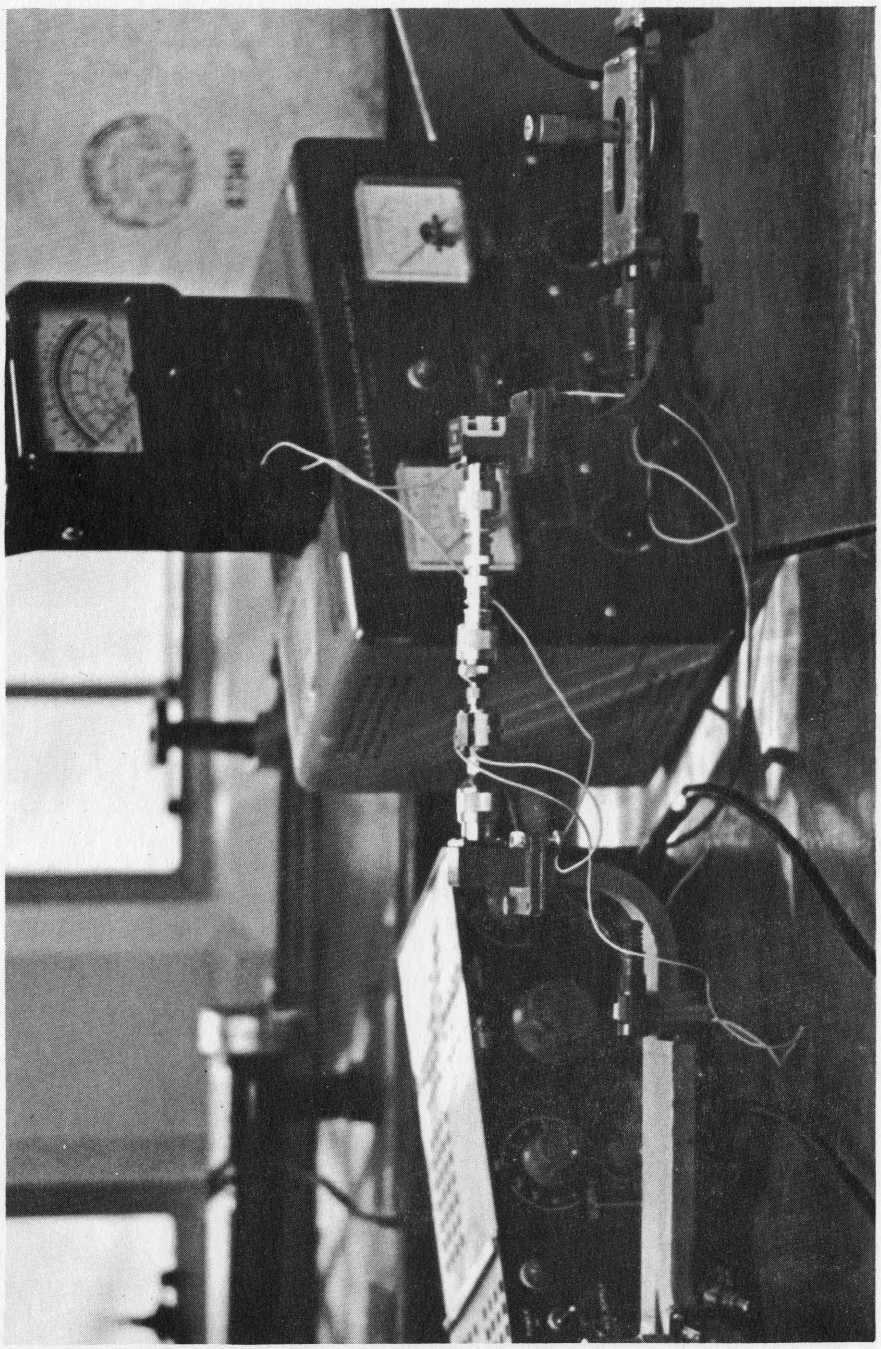

PLATE 3
HOLDER AND CONNECTORS

Determination Of DC Characteristics

The d-c characteristics of the active RC line were determined by using the Tektronix Curve Tracer and a VOM. Seven chips were available for testing and out of the seven, one was found to have the "best" characteristics. That is, it had a breakdown voltage of -45 volts. All the rest had breakdown voltages ranging between -3 volts and -20 volts. Since the one "good" chip used the separate bias fingers arrangement, it was also possible to find the values of the series resistance elements of the line. This was done both with the curve tracer and the VOM. The equivalent d-c circuit as seen by the VOM is shown in figure 10.

The ground return for the chip was the base of the header. The tab numbers started at the upper right-hand corner of the header as viewed from the top. It should be noted that the 750 ohm resistors in series with the diodes are not physical resistors. They are the resistance of the diodes in the forward conduction mode and decrease in value as forward current increases. These values were obtained from a low setting on the VOM (Rx10 scale). Since breakdown voltage was -45 volts instead of -75 volts as expected and the series resistors were 1.1-KΩ instead of 600 ohms (because of difficulties holding tight tolerances in fabrication), the $|R_1 G_2|$ product was not expected to be 0.3 but more like 0.1. The breakdown voltages of each of the diodes did

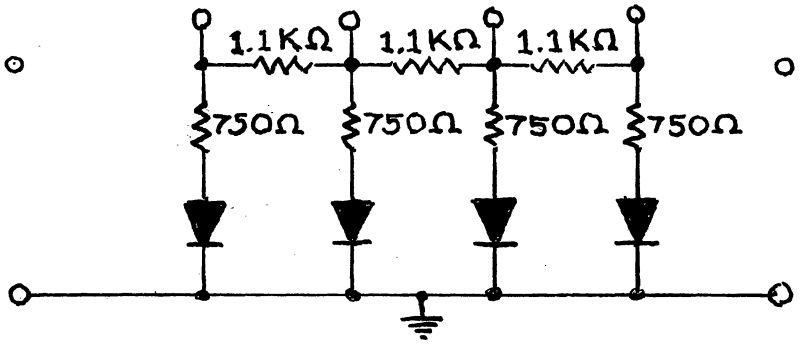

Fig. 10

Equivalent circuit as seen by VOM

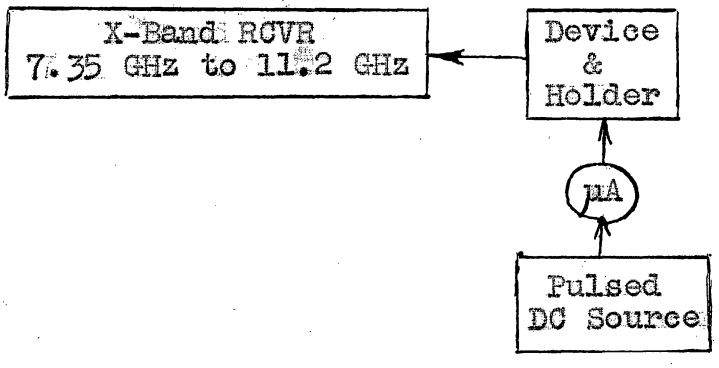

Fig. 11

Block diagram of set-up to detect oscillations

not differ more than a volt from the nominal value of -45 volts. With the d-c characteristics determined, a microwave bench set-up was devised to test the r-f characteristics of the line.

Testing For Open-Circuit Oscillations

The first r-f test on the device was to determine if open-circuit oscillations occurred. No signal was applied to the input and the device was biased into avalanche. The test set-up for this is shown in figure 11.

A pulsed bias source had to be used because the heat sinking of the chip was not efficient enough to allow continuous operation at the high current levels required (approximately 9 mA being considered a "normal" value for CW operation). Because this device had half the expected breakdown voltage, peak current through the device was limited to less than 5 mA to minimize overheating and burnup.

The pulsed d-c source consisted of a square-wave pulse generator (variable duty cycle and pulse width) and d-c power supply connected in series. The d-c supply had to be used because the pulse generator's voltage output could only go as high as 40 volts. The d-c supply provided a means of shifting the zero volt reference of the pulse generator in a negative direction in order to have the total voltage output of the combined supplies exceed the -45 volt breakdown of the diodes. A microammeter was connected in series with the voltage

supplies and the device to monitor the average value of the pulsed current.

To "calibrate" the microammeter (see if the indicated average value of current was the same as the calculated value) a 2-KΩ resistor was put in series with the meter and the voltage drop across the resistor was observed on an oscilloscope. The average value of the observed voltage divided by the 2-KΩ resistance was compared with the average value of current flowing through the meter and was found to agree fairly well. Thus, the meter could be used as an indicator of "safe" current levels. When it was necessary, the average current was found using the 2-KΩ resistor and oscilloscope for greater accuracy.

Since the input to the X-Band receiver used an N-type coaxial fitting, it was possible to connect the device directly to the receiver. This type of connection allowed a minimum loss of signal between device and receiver. The device was pulsed with peak currents ranging from 1 to 5 mA and the presence of oscillations was checked by slowly sweeping the receiver through its range. Even with the gain of the receiver set to maximum (which meant it was capable of detecting signal levels at around 0.05 mW), no indication of incoming r-f was observed on the db meter of the receiver. The lack of oscillations indicated that either the $|R_1 G_2|$ product of the line was such that oscillations could not occur or that the shunting admittances of header and

holder were such that they prevented oscillations ("detuned" the line).

Testing Transmission Quality

A check was next made on power transmission quality of the device both as a function of bias voltage and of frequency. The test set-up for this is shown in figure 12.

The power out versus bias voltage test was conducted on both types of chip. TABLE I is for data taken on the chip with the shorted biasing fingers. The plot of these data (figure 13) indicates that power transmission improves almost linearly with increasing reverse bias. A leveling off of output power change does occur near the point where avalanche is about to occur. This test was performed under matched-line conditions. Thus, for this type of chip, a 0.1 db improvement in power transmission was realized. Thus, the resistive diffusion extensions of the micro-strip lines did their job in improving transmission quality. No such effect was noted for the chip using the separate bias fingers arrangement. This result was to be expected since extension of the resistive diffusion was not used.

Data for transmitted power versus frequency was taken with the device in the passive mode. Again, everything was matched during this test. In order to find out how the chip performed by itself, a frequency response was taken on a "dummy" header first. The "dummy" was

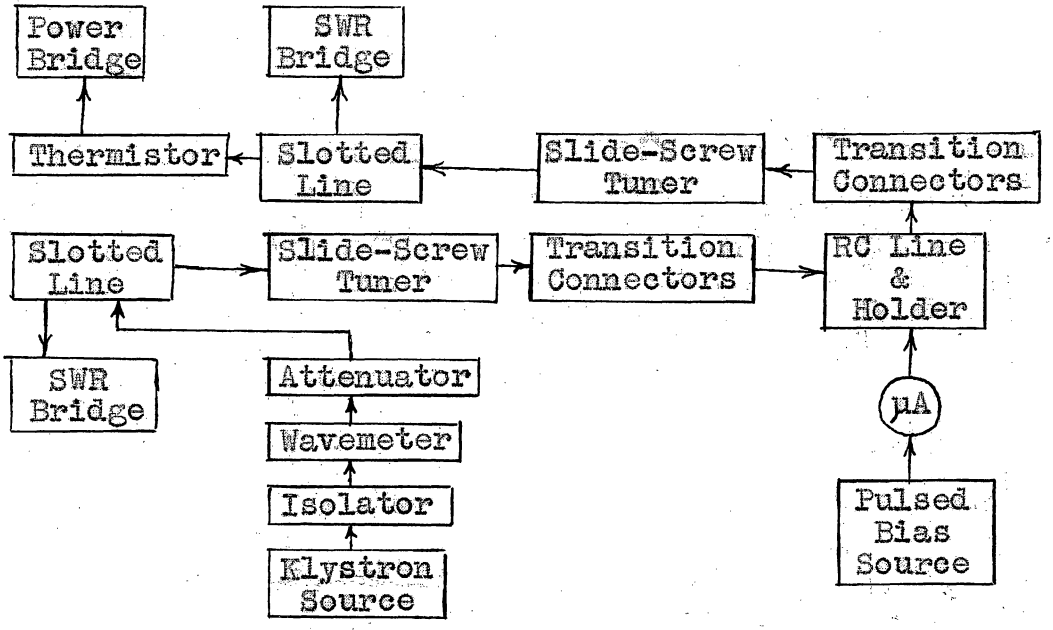

Fig. 12

Block diagram of test set-up to measure transmission quality

TABLE I

Data from power out versus bias voltage test

BIAS VOLTAGE (-V)	POWER OUT (mW)
0.0	1.0
6.3	1.01
10.2	1.015
12.5	1.018
18.0	1.02

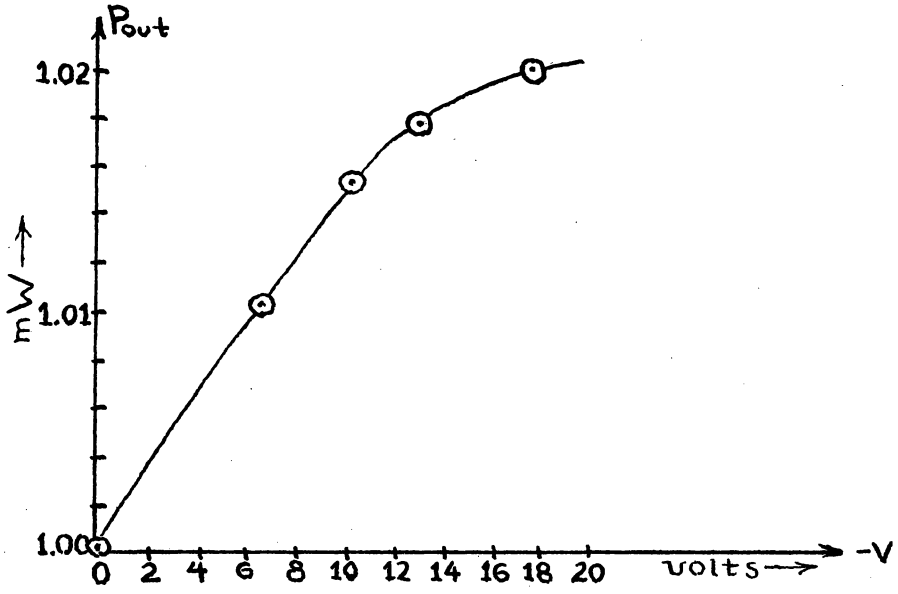

Fig. 13

Plot of output power versus bias voltage

constructed with the same type of header as used in the regular device with the exception that a straight piece of gold ribbon conductor was connected between input and output r-f tabs instead of a chip. Reference power into the dummy was 1 mW. TABLE II lists the data for this part of the test. A frequency response on the "good" chip was done next. TABLE III lists these results.

A graph was constructed from the data of these two tests. GRAPH I shows db loss for the "dummy" device, actual device, and the chip by itself (found by subtracting db losses of TABLE II from db losses of TABLE III). The graph shows that the combination of header and holder exhibit a resonance effect near 9.1 GHz and that the effect is like a series R-L-C circuit shunting the transmission line. Since this effect was observed with both the dummy header and the regular device, it appears to be the result of the physical design of header and holder and not of the chip itself. The "bandwidth" for the dummy unit (taken at its 7.5 db points) was 1.22 GHz; for the actual device (taken at its 9.1 db points) was approximately 0.88 GHz and for the chip alone (taken at its 4.3 db points) was approximately 1.18 GHz. These "bandwidths" are not to be confused with the actual operating bandwidth of the device. They merely show the range over which minimum power absorption was observed. If the chip has to operate outside of these ranges, then it has to have more gain to overcome the increased losses and still provide an amplified signal at the output.

TABLE II

Frequency response of "dummy" unit

FREQ (GHz)	POWER OUT (mW)	POWER LOSS (db)
8.680	.21	6.78
8.757	.24	6.20
8.800	.26	5.85
8.873	.29	5.38
8.967	.34	4.68
9.130	.24	6.20
9.178	.34	4.68
9.262	.34	4.68
9.388	.34	4.68
9.575	.32	4.95
9.641	.28	5.53
9.735	.21	6.78

TABLE III

Frequency response of actual unit

FREQ (GHz)	POWER OUT (mW)	POWER LOSS (db)
8.645	.12	9.21
8.750	.16	7.96
8.800	.20	7.00
8.875	.21	6.78
8.960	.24	6.20
8.973	.24	6.20
9.030	.24	6.20
9.050	.21	6.78
9.100	.12	9.21
9.130	.20	7.00
9.214	.22	6.58
9.317	.20	7.00
9.404	.15	8.24
9.462	.13	8.87
9.510	.12	9.21
9.590	.12	9.21
9.670	.09	10.46
9.727	.08	10.97

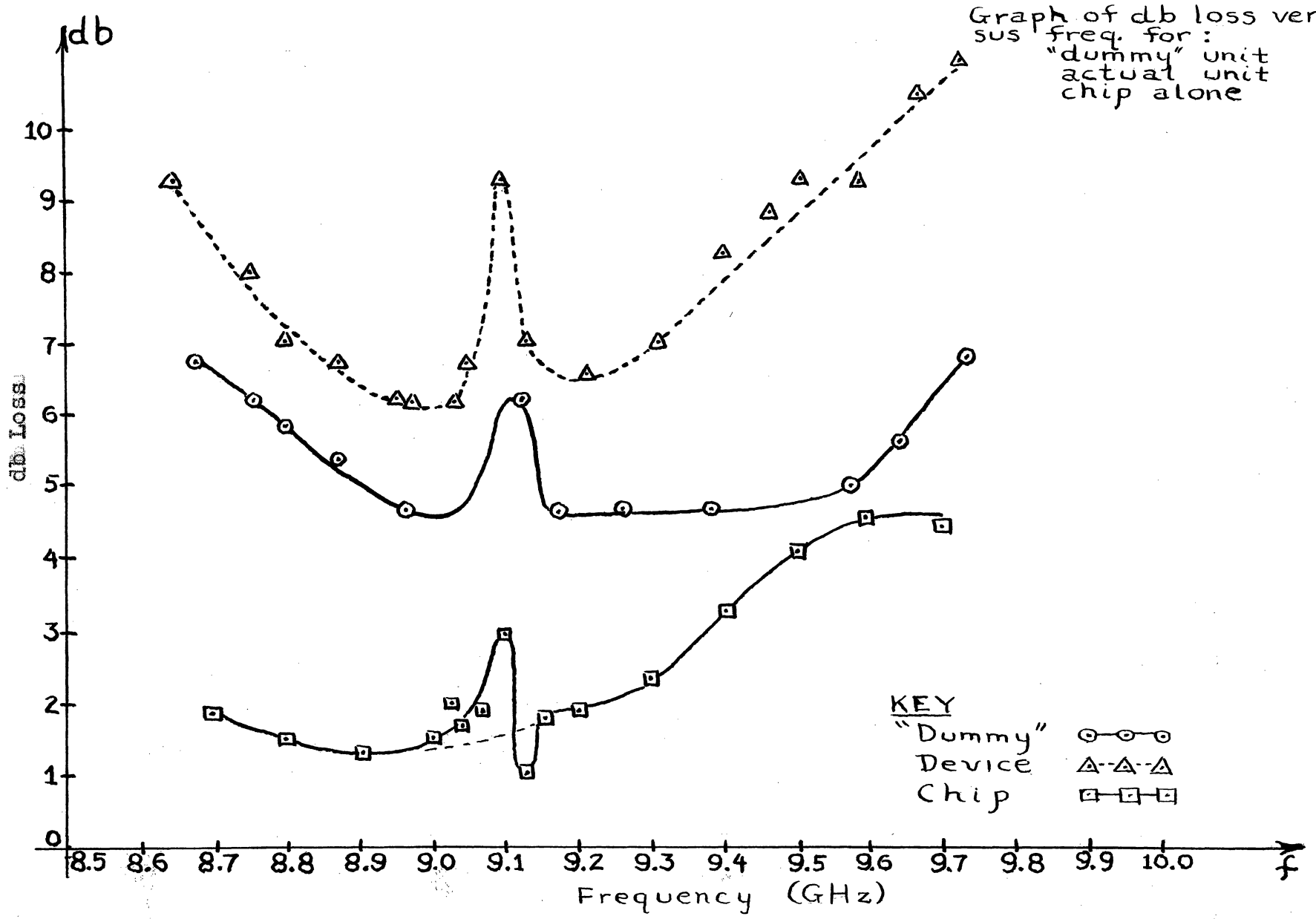
Graph of db loss versus freq. for:
"dummy" unit
actual unit
chip alone
db
db Loss
10
9
8
7
6
5
4
3
2
1
0
8.5
8.6
8.7
8.8
8.9
9.0
9.1
9.2
9.3
9.4
9.5
9.6
9.7
9.8
9.9
10.0
f
Frequency (GHz)
KEY
"Dummy"
Device
Chip

Fig. 14

The abrupt changes seen on the plot pertaining to the chip alone (near 9.1 GHz) are the result of the calculations in obtaining the plot and are not observed results. The dotted line through this region is more of what the author believes to be the true response of the chip. From this plot it is also apparent that the power loss in the chip is rather small compared to the losses of its header and holder.

Testing For Voltage Gain

In order to test the device for gain, the bench set-up was modified as shown in figure 15. This set-up could only be used to check the open-circuit voltage gain of the device. In order to check the device's gain under various load conditions a "line stretcher" or phase shifter terminated in some real resistance is required. However, this equipment was not available at the time of this experiment. On page 44 is a photograph of the bench set-up used.

Below is an outline of what was done to set up and test the device for gain.

I. Test Procedure

   A. Allowed a half-hour for equipment warm-up.

   B. Initial conditions

      1. Power thermistor replaced short

      2. No bias on the device

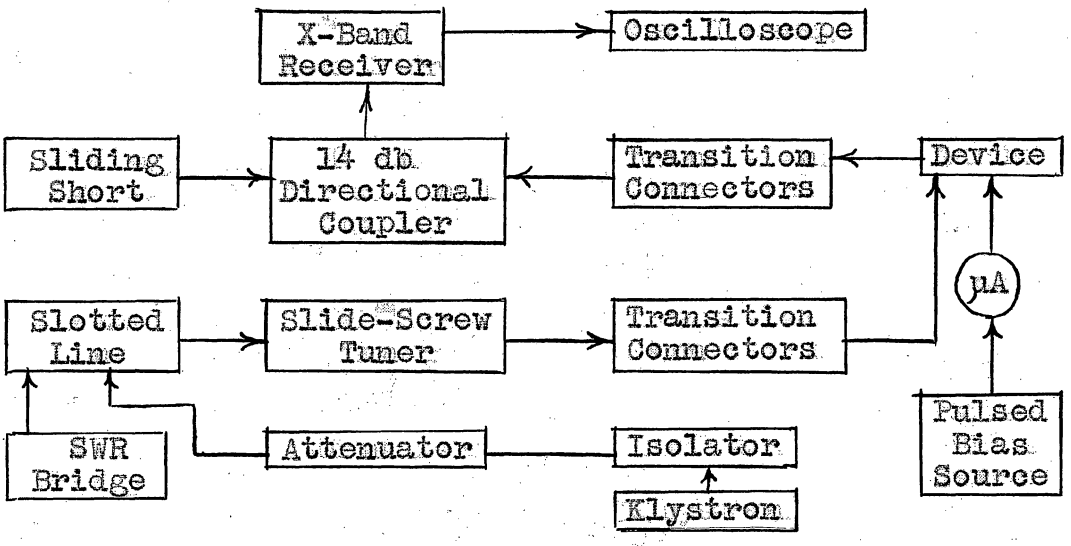

Fig. 15

Block diagram of bench set-up to check device's gain

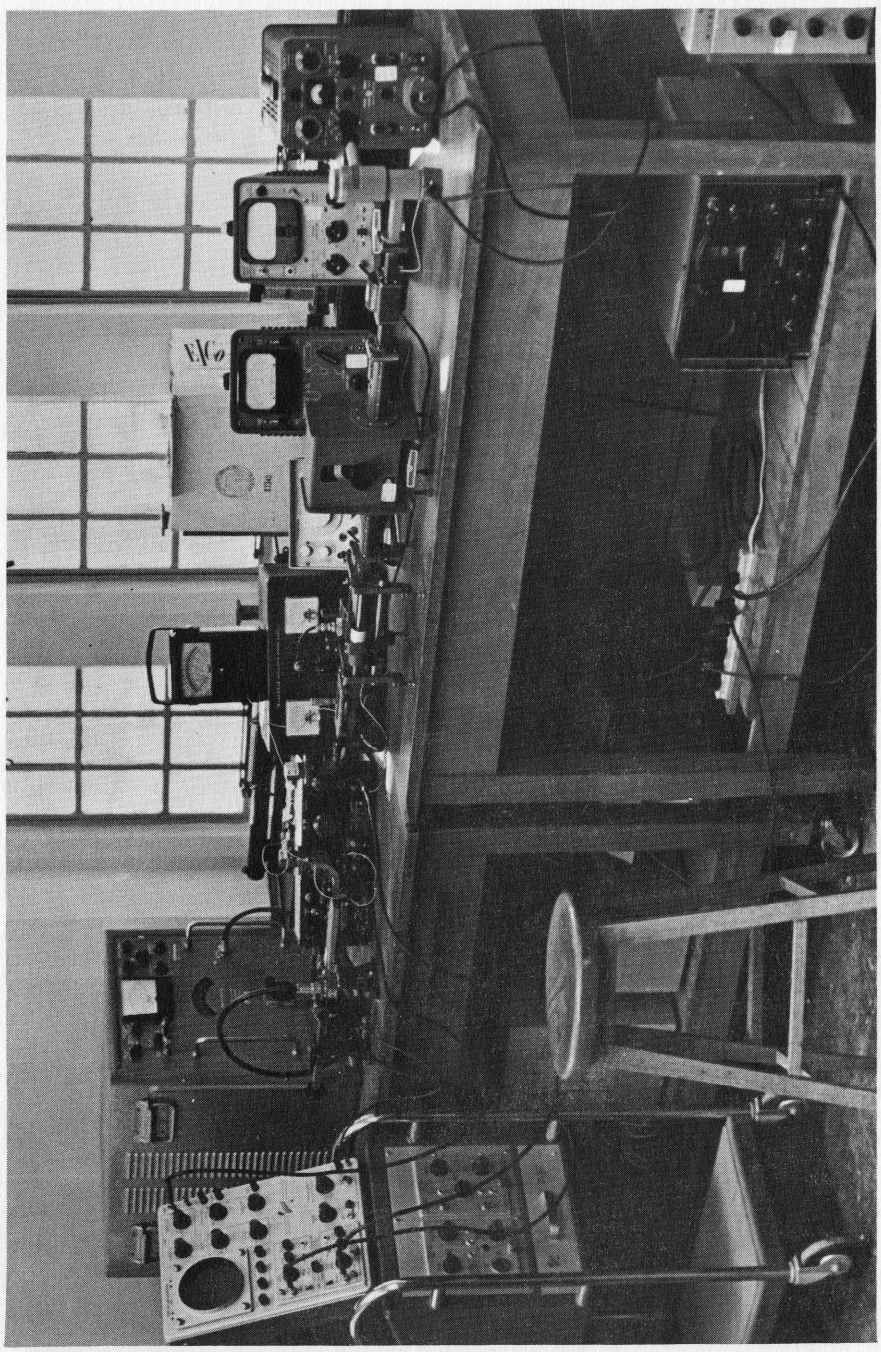

PLATE 4
COMPLETE ASSEMBLY

3. Klystron frequency set between 8.96 GHz to 9.03 GHz
4. Slide-screw tuner out of the line
5. Input power to device: 1 mW
6. X-Band receiver gains set to maximum; AVC in ON position

C. Inserted slide-screw tuner and adjusted it for a minimum SWR on the line. Since obtaining SWR measurements requires the klystron be modulated with a 1000 Hz signal, its power supply modulator had to be turned on. It was found that more noise was introduced when the modulator was on so after the tuner was adjusted, the modulator was shut off.

D. The microwave attenuator was adjusted for a 0.4 mW reading on the power bridge.

E. The pulse generator of the bias supply was set for a PRF of 1 Hz (obtained by externally driving it with the Wavetek VCG), a pulse width of 1 msec and a pulse amplitude of -40 volts. The d-c supply was adjusted for an output voltage of -45 volts.

1. At this point the microammeter was showing current pulses and the power meter was showing

periodic absorptions of power. (A drop of 0.01 mW of output power every time the device was pulsed "on")

F. The slide-screw tuner was adjusted so that the device began to put out more power than was put into it ("on-time" power was greater than "off-time" power). This adjustment was made on a trial-and error basis. It was found that at the end of adjustment, the capacitive post has been advanced into the guide about three turns from its initial position and has moved about a centimeter towards the device from its initial position. The power meter was showing upward deflections of between 0.01 to 0.02 milliwatts and the r-f input meter of the receiver showed about 0.1 db gain.

G. The thermistor was replaced with a sliding short which was adjusted to reflect an open at the output port of the device.

H. The slide-screw tuner was readjusted for a maximum indication of gain on the receiver's db meter (approximately 0.25 db of voltage gain)

Since the input meter of the receiver could not respond instantaneously to the square-wave type of changes in the input signal, it

coult not be used as an accurate measure of the actual open-circuit voltage gain of the device. A better indication of the actual gain was the detected video signal at the output of the receiver. To do this it was again necessary to modulate the klystron with the 1000 Hz signal. This, of course, introduced more noise into the system and made it more difficult to determine actual voltage gain but this was the best method that was available at the time. The detected video from the receiver was fed to one channel of a dual-trace oscilloscope and the output from the pulse generator was connected to the other channel. The oscilloscope was synchronized to the pulse generator also. Adjustments were made on the oscilloscope so that the observed traces looked like those depicted in figure 16. The PRF of the pulse generator was set to about 3 Hz and adjusted so that the pulses on the bottom trace slowly "walked" across the screen. In the figure, the "on" time of the device was during the first 1 msec of the top trace. As the pulses on the bottom trace moved out from underneath the "on" pulse of the top trace, a drop in signal level was detected (as shown). Due to receiver and klystron noise, it was difficult to determine the exact amount of signal change. The best approach seemed to be to take a number of readings and average them to obtain a final value of signal amplification. This method was used in determining gain as a function of frequency. These results are listed in Table IV.

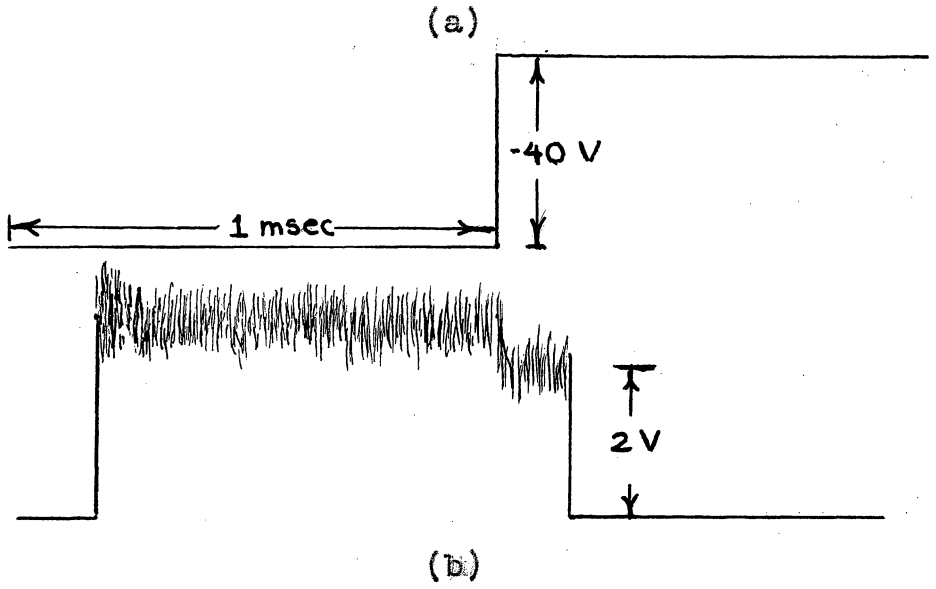

Fig. 16

Oscilloscope traces with (a) negative pulses from bias supply and (b) detected video from receiver

TABLE IV

Data for gain versus frequency

FREQ (GHz)	GAIN (voltage)	GAIN (db)
8.920	1.00	.00
8.940	1.08	.66
8.960	1.10	.82
8.973	1.11	.90
9.000	1.11	.90
9.030	1.10	.82
9.033	1.08	.66
9.040	1.00	.00

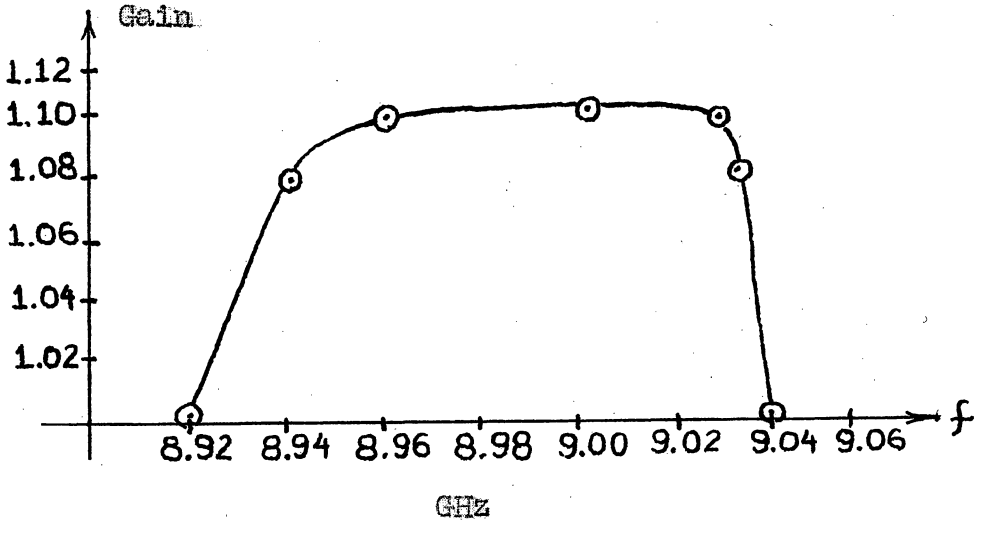

Fig. 17

Plot of open-circuit voltage gain as a function of frequency

A plot of gain versus frequency is shown in figure 17. From this plot it was determined that the "useful" bandwidth of this device is about 110 MHz. A rather sharp decrease in gain after 9.03 GHz is attributed to the resonance effect of header and holder. If this effect was eliminated, it seems possible that the bandwidth might be around 250 MHz (obtained by eliminating the resonance peak from the top curve on GRAPH I and reading the new 6.3 db intercepts).

Determination Of Open- and Short-Circuit Admittances

For this part of the testing, the equipment from the source end to the device stayed the same as shown in figure 15. No hardware was connected to the output end of the device. The open- and short-circuit admittances of the device were found by standard null-shift methods using a slotted line and SWR meter. Care was taken that the reference short was always as close to the chip as possible. For this purpose, a small piece of good conductor was shaped so that it could rest on a input or output r-f tab of the header and short them to ground when the pressure screws were screwed into place. The disadvantage of this method was that the holder assembly had to be taken apart and put back together for each test. This proved to be time consuming and prone to errors. Consequently, this test had to be run several times to see how much deviation occurred between like measurements.

Great care had to be taken each time the holder was reassembled in order to try and keep the r-f characteristics the same from test to test. The frequency used was 9 GHz. The device was biased as before. The Smith Chart was used to get the normalized admittances of the device. These were then multiplied by 0.02 mho (the OSM connectors have a Z_o of 50 ohms) to get the actual admittances. TABLE V lists these results. To get an idea of the input and output admittances of the chip by itself, the open- and short-circuit admittances of the dummy unit were found. Subtracting these values from those in TABLE V gave the admittances of the chip listed in TABLE VI.

The values of TABLE VI indicate that the chip "looked" like a negative conductance shunted by an inductance at the test frequency used. However, not too much significance can be placed on the numbers obtained because of difficulties encountered in conducting this part of the experiment.

One such difficulty was in reading the SWR on the line. Since all the readings were 5:1 or greater, all the readings fell outside the calibrated range of the SWR meter. Thus, they had to be estimated. The presence of system noise and the fact that the device was "on" for only short periods of time added to the difficulty. Each time the device was pulsed, the SWR meter would "jump" to a slightly lower reading. The noise bursts on the line were of equal or greater magnitude than the

TABLE V

Admittances of
total unit

SWR	NULL SHIFT	ADMITTANCE
5:1	.162 (to gen.)	$(Y_{in})_{oc} = .0056 - j.01152$ mho
5.5:1	.081 (to gen.)	$(Y_{in})_{sc} = .0130 - j.03160$ mho
5.5:1	.180 (to gen.)	$(Y_{out})_{oc} = .0044 - j.00900$ mho
5:1	.204 (to gen.)	$(Y_{out})_{sc} = .0044 - j.00526$ mho

Admittances of
dummy unit

$Y_{oc} = .0198 + j.0040$ mho

$Y_{sc} = .0080 + j.0016$ mho

TABLE VI

Admittances of
the chip

ADMITTANCE

$(Y_{in})_{oc} =$	$-.01420 - j.01552$ mho
$(Y_{in})_{sc} =$	$.00500 - j.03320$ mho
$(Y_{out})_{oc} =$	$-.01540 - j.01300$ mho
$(Y_{out})_{sc} =$	$-.00362 - j.00686$ mho

"jumps" so that the cumulative effect was a very erratic reading on the meter. An attempt was made to minimize these effects by visually averaging out the influence of noise on the meter readings and estimating what the SWR would be if the device was on all of the time. This estimation was based on the PRF and pulse duration during "on time" and the amount the SWR meter moved during this time.

Also, another source of error in these readings came from the fact that the device had to be taken apart and put back together for each reading. This introduced slight changes in the r-f characteristics of the holder each time this was done. Since a finite length of time would elapse during mechanical changes on the device, the klystron had a chance to drift in frequency. However, this source of error is not as significant as that due to noise.

Because of these difficulties, the only conclusions that can be drawn from these results is that a) the device does exhibit negative conductance effects in this frequency range b) the fact that the admittances had an inductive component implies that the test frequency was below the resonance frequency of the RC line.

A better scheme for obtaining admittance values would be to use an impedance plotter which uses a visual display of the Smith Chart on the face of its CRT. Each time the device was pulsed, the effect would register as a "bump" on the CRT trace and would give a more accurate display of the actual "on-time" admittance of the device.

Noise Characteristics

Due to time and equipment limitations, it was not possible to obtain a noise figure for the active RC line. All that was done was to observe the detected video output from the X-Band receiver and note if any increase in noise amplitude occurred during the "on time" of the device. At an operating frequency of 9 GHz and the device functioning as an amplifier, it was found that the magnitude of the "on-time" noise voltage was approximately 1.2 times the "off-time" noise voltage. Noise voltage distribution during "on time" was like that shown in figure 18.

The noise distribution can be correlated with bias current levels during "on time". It was found that current through the device as a function of time looked like that shown in figure 19. The "sag" in current was attributed to loading down of the bias supplies (they were not constant-current supplies). Comparing figure 18 with figure 19 reveals that the greatest amount of noise (and also the largest signal-voltage amplification) occurred during the highest current levels. This is what was expected. In general, the overall noise level did not increase very much for the current levels used.

Proximity Effects

Another problem which occurred in the testing of this device was the effect objects near the device had on it. Apparently the physical

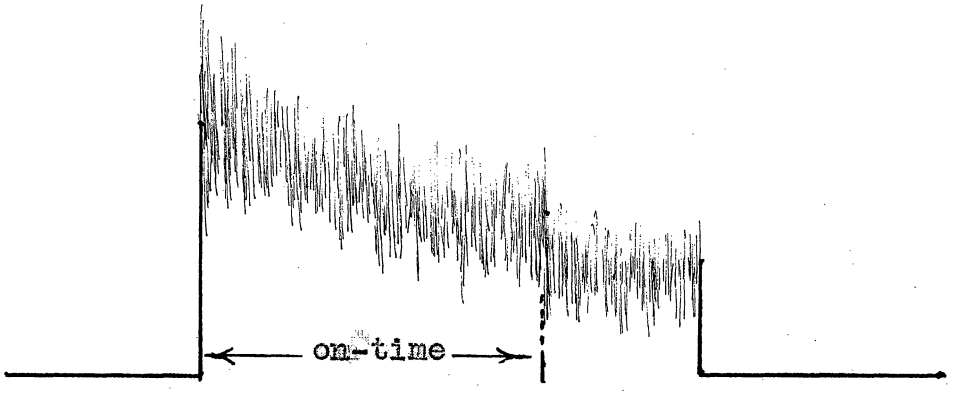

Fig. 18

Noise voltage distribution of detected signal

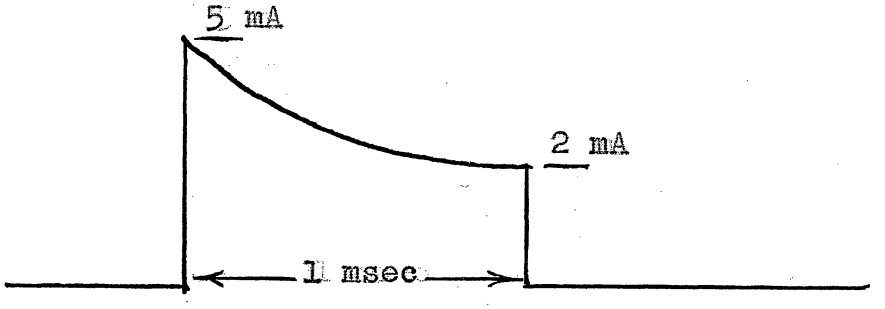

Fig. 19

Current amplitude during "on time"

construction of the device allowed a great deal of "r-f leakage" because any object moving within a six-inch radius of the device caused meter readings to fluctuate. To minimize this effect, the area around the device was kept as clear as possible and any adjustments or readings that had to be made near or on the device were made taking proximity effects into account.

CONCLUSIONS

The test program carried out on the active RC line and the results obtained have lead to the following conclusions. Because open-circuit oscillations were not detected, either the $|R_1 G_2|$ product was less than 0.1 or the reactive effects of header and holder were such as to prevent oscillations ("detuning" the RC line). Making the resistive diffusion extensions part of the micro-strip transmission lines lowered dielectric losses under reverse-bias conditions. Transmission losses due to header and holder are much greater than for the chip alone. This in turn, greatly reduces the operating range of the device. The open-circuit voltage gain of the device was comparable with that predicted by theory (i.e. theoretical gain $=$ 1.204; experimental gain $\cong$ 1.1). The device exhibits band-pass characteristics. Its effective bandwidth is approximately 110 MHz. It seems reasonable to assume that this bandwidth can be doubled by eliminating a resonance effect in the header and holder. Open- and short-circuit admittances of the device indicate the presence of negative conductance in the active RC line. Also, their reactive components indicate that the resonance frequency of the line is above 9 GHz (The original design called for a 10 GHz resonance frequency). Noise voltage produced by the IMPATT diodes is proportional to the bias current. At the current levels used in this experiment,

approximately 20% increase in "on-time" noise was detected.

It appears that this particular design of an active RC line has great potential as a microwave amplifier. What seems to be the biggest problem right now is to get a better design of the chip's header and holder (cut down losses and eliminate that resonance effect). The improved design plus refining the testing procedure should show that this device comes quite close to fulfilling theoretical predictions.

APPENDIX A

LISTING

```
1 FORMAT(2E11.5, I4)
2 FORMAT(1H1,10X.10HFOR RIN =  , E11.5,2X,15HAND FOR GAIN
    =  ,E11.5,2X,
 1  7H, RG = ,E11.5,2X,9HAND RL =  , E11.5)
  DIMENSION A(10,10)
(Read in network parameters and number of sections)
  READ 1, R1, R2, MM
(R1 is series resistance, R2 is negative shunt resistance, MM is
     the number of network sections)
(Read in desired input resistance and overall gain)
  READ 1,  RIN, AV
(Define matrix elements for one section of the network)
  A(1,1)=1.+R1/R2
  A(1,2)=R1
  A(2,1)=1./R2
  A(2,2)=1.
(Calculate matrix for MM sections of the network)
  CALL MTRX (A, A,  O)
  J=MM-2
```

```
  DO 10 I = 1, J
  CALL MTRX ( O,  A,  O)
10 CONTINUE
  DO 19 N = 1, 2
  DO 18 L = 1, 2
  Y( L,N) = O(L,N)
18 CONTINUE
19 CONTINUE
(Calculate the values of RL and RG)
  RL-( AV*Y(1,2))/(1.-Y(1,1)*AV)
  XX=(Y(2,1)*RL+Y(2,2))/(Y(1,1)*RL+Y(1,2))
  RG+RIN/(1.-RIN*XX)
  PRINT 2, RIN, AV, RG, RL
(Insert option cards for RL and RG here)
(Calculate gain and RIN for a given RL and RG)
  AV = RL/(Y(1,1)*RL + Y(1,2))
  RIN = RG/(1. + RG*XX)
  PRINT 2, RIN, AV, RG, RL
  STOP
  END
(Subroutine for multiplying two 2x2 matrices together. Output of this
 subroutine is another 2x2 matrix and uses the variable name 'O'.)
```

```
      SUBROUTINE MTRX(P, Q, O)
      DIMENSION P(10,10), Q(10,10), S(10,10), O(10,10)
      DO 15 K = 1, 2
      DO 14 I = 1, 2
      SUM = 0.0
      DO 13 J = 1, 2
      SUM = SUM + P(I,J)*Q(J,K)
   13 CONTINUE
      S(I,K) = SUM
   14 CONTINUE
   15 CONTINUE
      DO 17 I = 1, 2
      DO 16 J = 1, 2
      O(I,J) = S(I,J)
   16 CONTINUE
   17 CONTINUE
      RETURN
      END
```

SAMPLE DATA

From design data on the active RC line

R1 = 600 ohms, R2 = -2000 ohms

Given: RIN = 50 ohms, GAIN (AV) = 100

Find: RG and RL

Computor answers: RG = 7.6588 ohms, RL = 1079.6 ohms

Given: RG = 100 Megohms, RL = 100 Megohms

Find: RIN and AV

Computor answers: RIN = -9.0442 ohms, AV = -1.2035

NOTE: The above data was compared to the exact solutions of the network equations and found to be the same.

REFERENCES

1. Read, W. T., Jr., "A proposed high-frequency, negative-resistance diode", Bell System Tech J. vol. 37, pp. 401-446, March 1958

2. Misawa, T., "Negative resistance in p-n junctions under avalanche breakdown condition, Part II", IEEE Trans. Electron Devices ED-13, pp. 143-151, January 1966

3. DeLoach, B. C., and Johnston, R. L., "Avalanche transit-time microwave oscillators", IEEE Trans. Electron Devices ED-13, pp. 181-186, January 1966

4. Kabaservice, T. P., "An integrated, microwave-frequency active RC line", United Aircraft Research Laboratories Internal Research Report, UAR-F154, pp. 1-16, August 31, 1967

The vita has been removed from the scanned document

ABSTRACT

This thesis is a report on an experimental study done on a new type of microwave device. This device is a monolithic, integrated circuit which uses "lumped" elements to approximate a distributed-parameter active RC line. The active regions of this device are IMPATT diodes which are capable of generating negative conductance effects (through transit-time delays of majority carriers) at microwave frequencies. The combined effect of negative conductance and positive real resistance within the device makes it capable of being a microwave amplifier or oscillator. The advantage of this type of device is that it does not have to present a negative impedance to an external signal source (as is the case with parametric amplifiers) to accomplish gain. Due to the nature of its design, it is inherently more "broadbanded" than the parametric amplifier. Also, no external "pump" is needed since the device obtains gain by an entirely different principle.

In the following pages a brief description of the basic operating theory of the device will be given. This description will show how the negative conductance effect is generated and how this is incorporated into the design of the final active network. Following this is a detailed discussion of experimental procedure, device characteristics sought, and the results obtained. The results of testing show that this device is capable of functioning as a microwave amplifier. They also show

that more work will have to be done in improving the "packaging" of the device. Aside from these "packaging" problems, it appears that this device is the key to a new area of microwave semiconductor devices.